J Mater Sci: Mater Med (2008) 19:965–974
DOI 10.1007/s10856-007-3351-8

Analysis of OPLA scaffolds for bone engineering constructs using human jaw periosteal cells

Dorothea Alexander · Jürgen Hoffmann · Adelheid Munz · Björn Friedrich · Jürgen Geis-Gerstorfer · Siegmar Reinert

Received: 1 September 2007 / Accepted: 5 December 2007 / Published online: 25 December 2007

Abstract For bone regeneration constructs using human jaw periosteal cells (JPC) the extent of osteoinductive ability of different three-dimensional scaffolds is not yet established. We analyzed open-cell polylactic acid (OPLA) scaffolds for their suitability as bone engineering constructs using human JPC. Cell adhesion and spreading was visualized on the surface of scaffolds by scanning electron microscopy. JPC proliferation within OPLA scaffolds was compared with proliferation within collagen and calcium phosphate scaffolds. We found a significant increase of proliferation rates in OPLA scaffolds versus Coll/CaP scaffolds at three time points. Live-measurements of oxygen consumption within the cell-seeded scaffolds indicate that the in vitro culturing time should not exceed 12–15 days. OPLA scaffolds, which were turned out to be the most beneficial for JPC growth, were chosen for osteogenic differentiation experiments with or without BMP-2. Gene expression analyses demonstrated induction of several osteogenic genes (alkaline phosphatase, osterix, Runx-2 and insulin-like growth factor) within the 3D-scaffolds after 12 days of in vitro culturing. Element analysis by EDX spectrometry of arising nodules during osteogenesis demonstrated that JPC growing within OPLA scaffolds are able to form CaP particles. We conclude that OPLA scaffolds provide a promising environment for bone substitutes using human JPC.

D. Alexander (✉) · J. Hoffmann · A. Munz · S. Reinert
Department of Oral and Maxillofacial Surgery, University Hospital Tübingen, Osianderstr. 2-8, 72076 Tubingen, Germany
e-mail: dorothea.alexander@med.uni-tuebingen.de

B. Friedrich
Department of Internal Medicine IV, University Hospital Tübingen, Otfried-Müller-Str. 10, 72076 Tubingen, Germany

J. Geis-Gerstorfer
Department of Prosthodontics, Section Medical Materials and Technology, University Hospital Tübingen, Osianderstr. 2-8, 72076 Tubingen, Germany

1 Introduction

Tissue engineering combines the use of suitable cells and supportive bioresorbable three-dimensional scaffolds to repair tissue defects. The use of biodegradable three-dimensional (3D) scaffolds seeded with bone progenitor cells may be an excellent alternative to the transplantation of autologous bone. From a clinical point of view, a resorbable scaffold allows monitoring bone formation by conventional X-rays or computer tomography, whereas a non- or slow-resorbable scaffold remains at the same density for a long time and avoids exact detection of newly formed bone. Periosteum-derived cells show stem cell potential by their capacity to form bone and cartilage in vitro and in vivo [1–4] These cells may be the first contributors together with osteoblasts in driving the cell differentiation process of bone repair [5].

A variety of natural and synthetic scaffold materials have already been investigated for bone tissue engineering including fibrin, hyaluronic acid, collagen gels and sponges, degradable polymers such as polylactides and polyglycolides, ceramics such as hydroxyapatite, tricalcium phosphate, coral and bioactive glass [6–14]. A typical porosity of 90% as well as a pore diameter of at least 100 μm seems to be advantageous for cell penetration and angiogenesis of the ingrown tissue [15, 16]. The variety of commercially available biomaterials for tissue engineering is continually expanding. For bone regeneration constructs using human jaw periosteal cells (JPC) the extent of

osteoinductive ability of different three-dimensional scaffolds is not yet established.

In the present study, we analyzed the suitability of commercially available 3D open-cell polylactic acid (OPLA) scaffolds for the growth and osteoinductive potential of human jaw periosteal cells using proliferation assays, scanning electron microscopy, real-time oxygen consumption measurements and EDX spectrometry. Furthermore, osteoinductive effects of OPLA scaffolds were also examined by analysis of gene expression in seeded JPC using quantitative real-time PCR.

2 Materials and methods

2.1 Human jaw periosteal cell cultures

Biopsies of human jaw periosteum were obtained during maxillofacial routine interventions. Samples from eight donors were included in the study in accordance with the local ethical committee, following informed consent. Jaw periosteal cells (JPC) were isolated in a pre-digestion step by type XI collagenase (1500 U/mL, Sigma, Steinheim, Germany) and dispase II (2.4 U/mL, Roche Applied Sciences, Mannheim, Germany) in a 1:1 mixture for 30 min. The main digestion step followed for 90 min with type XI collagenase.

JPC were cultured in D-MEM: F-12 (Invitrogen-BioSource Europe, Nivelles, Belgium) containing 10% FCS (Sigma-Aldrich, Steinheim, Germany), 100 U/mL penicillin/streptomycin (Cambrex, Walkersville, USA) and 50 µg/mL fungicide (Biochrom AG, Berlin, Germany). Periosteal cells from fourth to seventh passage were used for these experiments.

Because of the potential contamination of periosteal cells by fibrous tissue, cells firstly underwent a differentiation test in the 2D cell culture system. Mineralization of periosteal cells was detected by alizarin staining (data not shown). Only alizarin-positive JPC were included in this study.

2.2 Three-dimensional scaffolds

In contrast to conventional 2D cell culture systems, scaffolds provide an adhesive substrate that also serves as a 3D physical support matrix for in vitro cell culture. The 3D collagen composite scaffold (Coll) is a natural scaffold from a mixture of type I and III collagens derived from bovine hide. The 3D open-cell polylactic acid scaffold (OPLA) is a synthetic polymer scaffold, that is synthesized from D,D-L,L polylactic acid. This material has an open-cell facetted architecture, which is effective for culturing high density cell suspensions. The calcium phosphate scaffold (CaP) is a mineralized calcium phosphate bioceramic 3D construct. All scaffolds were provided from BD Biosciences (Bedford, USA). The average pore size of Coll and OPLA scaffolds measured 100–200 µm and 200–400 µm for the CaP constructs. OPLA and CaP, but not Coll scaffolds were noncompressible. All constructs measured a diameter × height of approximately 5 mm × 4.5 mm and a volume of 0.039 cm^3.

Scaffolds were pre-incubated with FCS-containing medium in a 96-well culture plate for one hour at room temperature. After removing the medium, the same cell number (5×10^4 cells) in a volume of 50 µL was seeded on the top of all analyzed scaffolds and incubated for 2 hours at 37 °C to allow cell adhesion. After this incubation time, additional 150 µL medium was added to the wells. For the following proliferation and differentiation assays, scaffolds were moved in fresh 96-well culture plates or for the oxygen measurements in fresh 24-well sensor dishes.

2.3 JPC proliferation assays within Coll, OPLA and CaP scaffolds

For the examination of JPC viability and proliferation, the commercially available kit EZ4U was used (Biozol, Eching, Germany). This test is based on the reduction of tetrazolium salts into formazan derivates by intact mitochondria. The quantification of this assay denotes the metabolic capacity of the cells.

JPC were seeded into different 3D-scaffolds and proliferation rates were analyzed after day 3, day 8 and day 14. For each analyzed patient ($n = 5$), optical densities from two cell-seeded scaffolds for each time point, were averaged.

2.4 JPC proliferation assays within OPLA 3D-scaffolds after induction of osteogenesis

Whereas JPC proliferation was analyzed within different biomaterials and OPLA scaffolds showed to be the most suitable scaffold for efficient proliferation of this stem cell type, we chose this material for further investigations. JPC proliferation rates within OPLA scaffolds were examined under three different culture conditions: (1) untreated: D-MEM: F-12 (Invitrogen-BioSource Europe, Nivelles, Belgium) containing 10% FCS (Sigma-Aldrich, Steinheim, Germany); (2) treated with osteoblast-medium (OB-medium) containing β-glycerophosphate (10 mM, Sigma-Aldrich), dexamethasone (1 µM, Sigma-Aldrich), L-ascorbic acid 2-phosphate (50 µM, Sigma-Aldrich); (3) treated with

osteoblast-medium and bone morphogenetic protein 2 (100 ng/mL, Cell Systems, St Katharinen, Germany) (OB/BMP-2). Proliferation rates were analyzed after day 3, day 8 and day 14. For each analyzed patient ($n = 3$), optical densities from two cell-seeded scaffolds for each time point and culture condition, were averaged.

2.5 Scanning electron microscopy and EDX analysis of JPC-seeded 3D-scaffolds

JPC attachment and spreading degree within Coll, OPLA and CaP scaffolds was visualized by scanning electron microscopy (SEM) ($n = 3$). Briefly, fixation of JPC on scaffolds followed with glutaraldehyde (2%) in 1 mM cacodylic acid Na salt (pH 7.4) for 60–90 min. After washing with distilled water, an ethanol ascending sequence followed, each step for 10 min. For gentle drying of the cell-seeded scaffolds, we utilized the critical point drying technique to avoid damage or severe collapse of surface structures. For scanning electron micrographs using the LEO 1430 (Zeiss, Oberkochen, Germany), cell-seeded scaffolds were sputter coated with gold/palladium. EDX (energy dispersive X-ray) analysis was performed using the Roentec UHV-Si(Li)-Detector (Roentec, Berlin, Germany).

2.6 Real time oxygen consumption measurements of JPC-seeded 3D-scaffolds

Real-time oxygen consumption measurements through proliferating JPC within Coll, OPLA and CaP scaffolds ($n = 3$) were performed using a suitable 24-channel SensorDish Reader (Presens, Regensburg, Germany). Oxygen concentrations (in scaffold supernatants) were permanently measured every 15 min within the sensor dishes containing the cell-seeded 3D-scaffolds. Altogether, oxygen measurements spanned 15 days of in vitro culturing.

2.7 Detection of alkaline phosphatase protein within JPC-seeded OPLA-scaffolds

Protein expression of alkaline phosphatase in JPC-seeded OPLA-scaffolds was detected after 13–14 days of in vitro culturing using a commercially available kit (Sigma-Aldrich, Steinheim, Germany) as recommended by the manufacturer ($n = 3$). Briefly, cell-seeded OPLA-scaffolds were shortly washed with PBS and incubated with the alkaline-naphthol mixture for 30 min in the dark. After subsequent washing, stained 3D-constructs were photographed.

2.8 RNA extraction from JPC-seeded OPLA-scaffolds

Automated disruption and homogenization of the JPC-seeded three-dimensional OPLA-scaffolds was established using the MagNa Lyser Instrument (Roche Diagnostics, Mannheim, Germany). The basic principle for cell disruption is the fastmoving, oscillating reciprocal motion of the MagNA Lyser Instrument rotor in which the MagNA Lyser ceramic beads filled with scaffolds and lysing reagents are loaded. The cell disruption process during a run with the MagNA Lyser Instrument is caused by the collision of ceramic beads with the sample within the sample tubes.

In detail, one-way special tubes with ceramic beads were filled with 700 µL of RLT-buffer (lysing buffer, Qiagen, Hilden, Germany) and 2–3 cell-seeded scaffolds. For each culture condition (untreated, treated with OB-medium or OB/BMP-2) extracted RNA from 5 scaffolds was pooled for sufficient RNA yield. Disruption and homogenization was performed by 6,500 rpm for one min. Cleared cell lysate was transferred in a fresh tube after short centrifugation for further RNA purification.

Total cellular RNA was extracted from untreated and differentiated JPC in the absence or presence of recombinant BMP-2 using the RNeasy Mini Kit (Qiagen, Hilden, Germany) as recommended by the manufacturer. First-strand cDNA for the real-time PCR experiments was synthesized by reverse transcription at 42 °C in a 20 µL reaction mixture containing 1 µg of total RNA. After heating the samples at 95 °C for 10 min. for denaturation and cooling to 4 °C, cDNA was used for PCR amplification. Reactions were diluted to 100 µL with DEPC treated water.

2.9 Analysis of gene expression by quantitative real-time PCR

Gene expression analyses were performed after 12 days of differentiation with OB-medium/OB-medium + BMP-2 in comparison to untreated cells. To quantitate mRNA expression, real-time PCR with the LightCycler System (Roche Applied Science, Mannheim, Germany) was established. Briefly, PCR reactions for GAPDH and the osteogenetic genes alkaline phosphatase, osterix, Runx-2 and insulin-like growth factor were performed in a final volume of 20 µL containing 2 µL cDNA, 2 µL primer mix (commercial primer kits from Search LC, Heidelberg, Germany), 2 µL DNA Master Sybr Green I mix (Roche Applied Sciences, Mannheim, Germany) and 14 µL DEPC treated water. Amplification of the target DNA was performed during 35–38 cycles of 95 °C for 10 s, 68 °C for 10 s and 72 °C for 16 s, each with a temperature transition rate of 20 °C/s and a secondary target temperature of 58 °C

Table 1 Induction of gene expression in differentiating compared to untreated JPC growing within OPLA scaffolds ($n = 3$)

Induction of genes during 3D-osteogenesis					
Pat no	Treatment	Alk. phosphatase	Osterix	Runx-2 (Cbfa1)	Insuline-like growth factor-2
#1	OB	20-fold	1.2-fold	2.2-fold	23.3-fold
	OB/BMP-2	20-fold	32-fold	4.1-fold	34.2-fold
#2	OB	4-fold	Nd	3.7-fold	12.5-fold
	OB/BMP-2	4-fold	15.4-fold	6.3-fold	22-fold
#3	OB	6.4-fold	0.68-fold	1.6-fold	4.3-fold
	OB/BMP-2	6.1-fold	3.25-fold	2.3-fold	6-fold

Gene expression in differentiating (OB, OB/BMP-2) versus untreated JPC growing within OPLA scaffolds was analyzed by quantitative PCR after 12 days of in vitro culturing. nd = not detectable. Induction indices of transcription levels in comparison to untreated controls (=1) are listed in the table

with a step size of 0.5 °C. Melting curve analysis was performed at 95 °C 0 s, 58 °C 10 s, 95 °C 0 s to allow discrimination between unspecific primer dimers and specific PCR products. The transcript levels of the housekeeping gene GAPDH were also determined for each sample using specific commercial primer kits (Search LC, Heidelberg, Germany). Finally, results were calculated as a ratio of the target versus house keeping gene transcripts. Induction indices of above mentioned genes from treated cells (OB-medium/OB-medium + BMP-2) in comparison to untreated cells are listed in Table 1.

2.10 Statistical analysis

Data are expressed as means ± SEM. Statistical analysis was performed using non-parametric paired/non-paired *t*-tests for data with a normal distribution. A value of $P < 0.05$ was considered as significant.

3 Results

3.1 JPC proliferation of Coll, OPLA and CaP scaffolds

Three days after seeding of JPC into different biomaterials, significant differences between the collagen, OPLA and CaP scaffolds were observed (Fig. 1a). JPC proliferation was 1.77-fold ($*P < 0.05$) increased within OPLA scaffolds in comparison to collagen scaffolds and 2.66-fold ($*P < 0.005$) higher than within CaP 3D-constructs ($n = 5$). 8 days after in vitro culturing, proliferation rates within OPLA scaffolds remained significantly higher (OPLA versus Coll 2.5-fold $*P < 0.001$ and OPLA vs CaP 3-fold $*P < 0.001$, $n = 5$) compared to the cell-seeded collagen and CaP constructs (Fig. 1b). At this time point, JPC seeded on collagen and calcium phosphate showed nearly the same proliferation rates. At day 14, the same tendency concerning JPC proliferation within OPLA in comparison to Coll scaffolds could be observed (Fig. 1c). JPC proliferation within CaP constructs seemed to overtake optical densities measured within collagen scaffolds at this time point however, no significant values could be obtained.

3.2 Scanning electron micrographs (SEM) of JPC-seeded 3D-scaffolds

JPC revealed a homogeneous colonization of the different biomaterials at a high density (200-fold magnification, Fig. 2). However, SEM visualization of growing JPC showed different morphology: cells growing within collagen scaffolds showed rather a roundish shape (Fig. 2a), whereas cell colonization of OPLA scaffolds was so dense, that only a uniform cell layer and not the single cell morphology was observed (Fig. 2b). Cells growing within CaP scaffolds revealed a flat shape (Fig. 2c).

3.3 Real-time oxygen consumption measurements of JPC-seeded 3D-scaffolds

Real-time measurements of JPC oxygen consumptions within the different biomaterials (measured in the scaffold supernatant) spanned 15 days of in vitro culturing. At the beginning of the experiment, the initial O_2-concentrations yielded average values between 79.5–83% ($n = 3$). Over the time course of the experiment, O_2-concentration constantly decreased through the proliferating cells until day 12–14. At this time point O_2-concentrations decreased significantly on average to 8.52 ± 1.48% ($*P < 0.005$) in

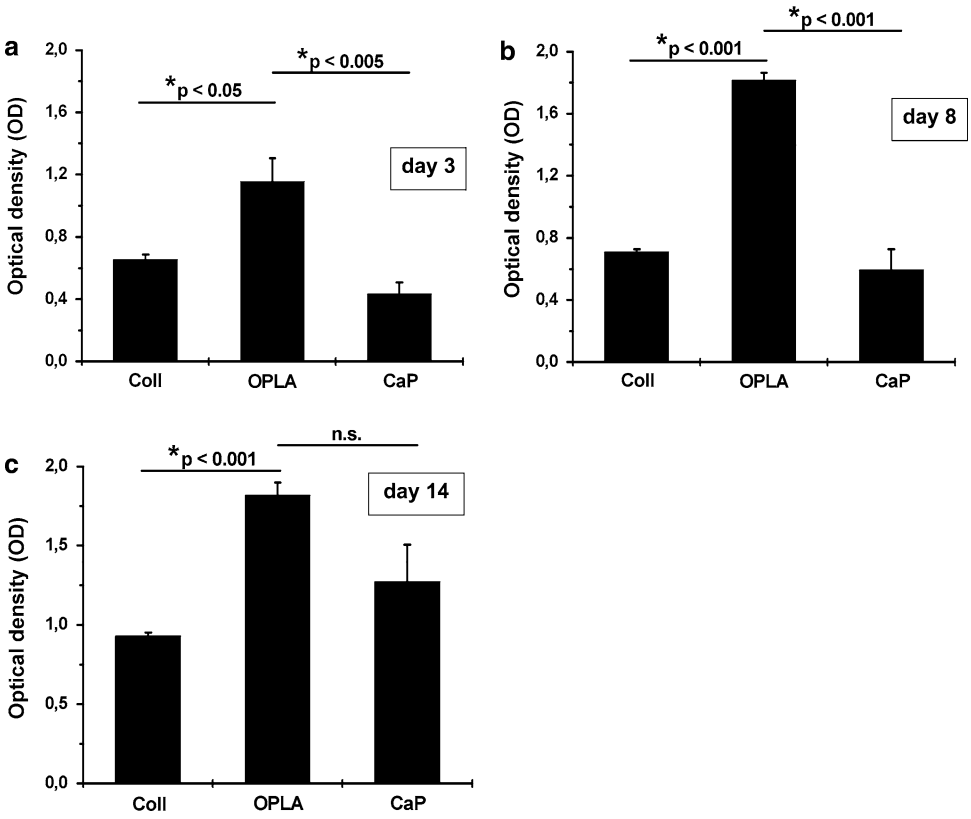

Fig. 1 JPC proliferation rates within Coll, OPLA and CaP scaffolds ($n = 5$). JPC were seeded into different biomaterials and proliferation rates were measured after day 3 (**a**), day 8 (**b**) and day 14 (**c**) of in vitro culturing by a colorimetric assay. Optical densities (OD) are denoted in the Y-axis

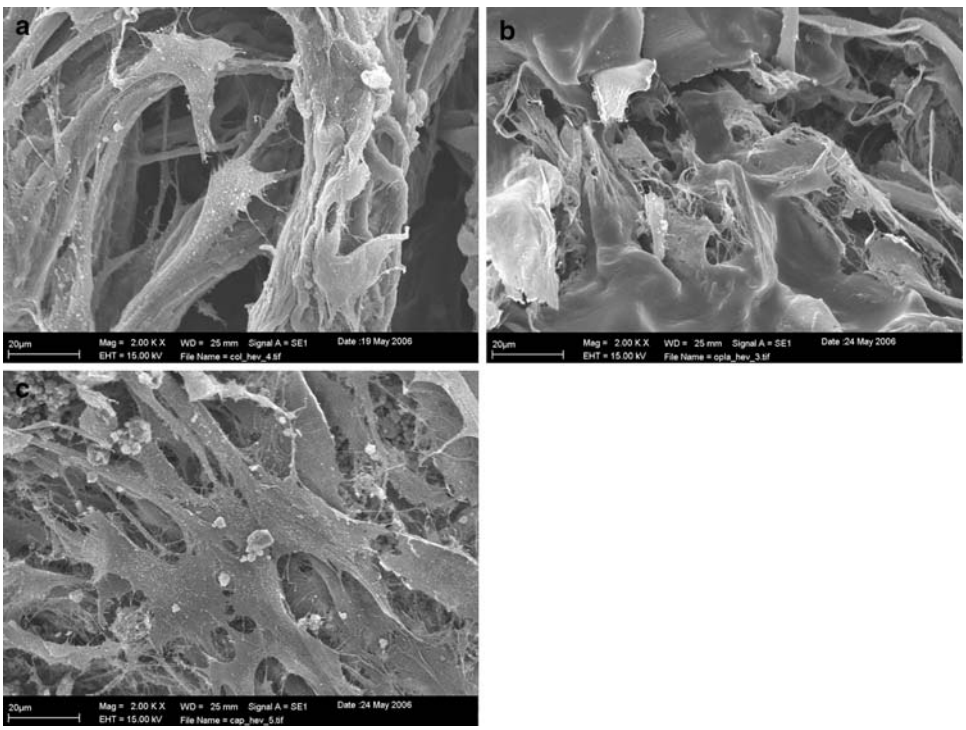

Fig. 2 Scanning electron micrographs (SEMs) of cell-seeded scaffolds ($n = 3$). JPC were seeded into Coll (**a**), OPLA (**b**) and CaP (**c**) biomaterials. Cell adhesion and spreading was visualized by SEM (200-fold magnification)

JPC-seeded collagen scaffolds in comparison to initial values (Fig. 3a), 6.6 ± 1.18% (*$P < 0.001$) in JPC-seeded OPLA scaffolds (Fig. 3b) and 5.9 ± 0.95% (*$P < 0.0001$) in cell-seeded CaP scaffolds (Fig. 3c). After day 14, O_2-concentrations were slightly increasing again.

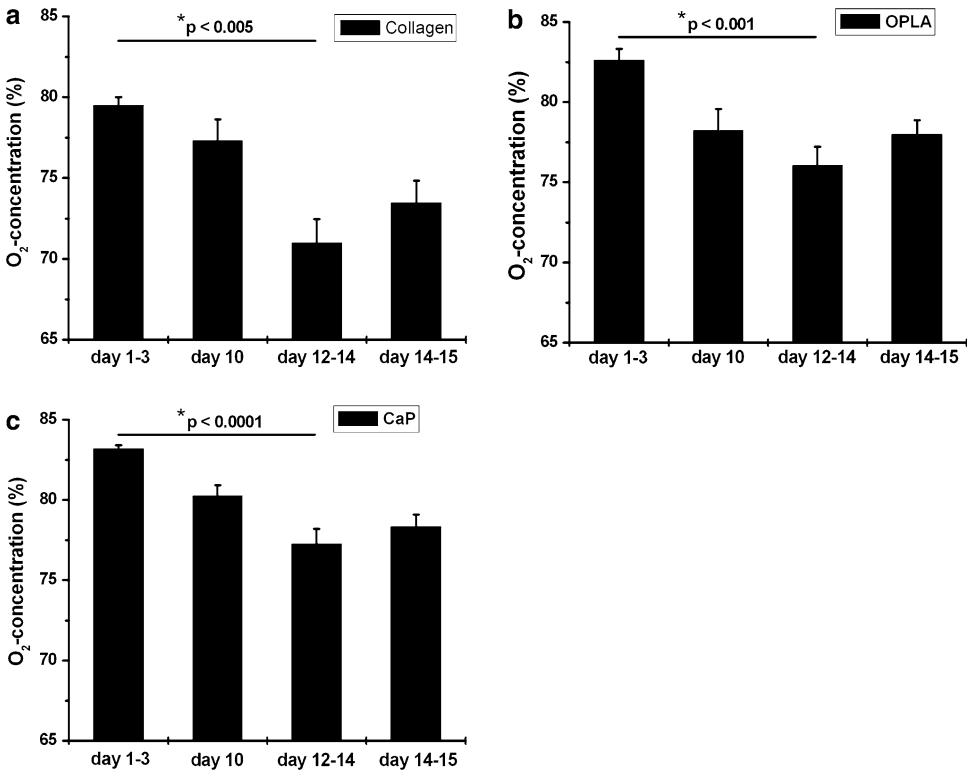

Fig. 3 Live-measurements of oxygen consumption through proliferating JPC within collagen, OPLA and CaP scaffolds ($n = 3$). Cell-seeded scaffolds were put into suitable sensor dishes and oxygen concentrations were permanently measured every 15 min. using a 24-channel SensorDish Reader. Live-measurements spanned 15 days of in vitro culturing

3.4 JPC proliferation assays and scanning electron micrographs (SEM) of JPC-seeded OPLA scaffolds after induction of osteogenesis

Examination of JPC proliferation under three different culture conditions within OPLA scaffolds showed a stimulating effect of OB-medium and an additional effect of OB/BMP2 ($n = 3$). After 3 days of JPC growing within OPLA scaffolds, JPC stimulated with OB-medium and additionally with BMP-2 showed higher proliferation rates than the other two groups (untreated and OB-medium, Fig. 4a). Eight days after initiation of osteogenesis, proliferation rates of BMP-2 activated cell group fell under the measured values from the untreated and OB-treated cells (Fig. 4b). At this time point JPC treated only with OB-medium showed the highest proliferation rates. After 14 days of differentiation, we found the highest proliferation in untreated JPC (Fig. 4c). However, differences in proliferation rates of the three analyzed groups did not reach significant values at any time point.

SEM visualization from untreated and differentiated JPC seeded within OPLA scaffolds were performed using the LEO 1430 electron microscope. Representative electron micrographs showed a weaker colonization of OPLA scaffolds when JPC were cultured in standard medium (Fig. 5a) in comparison to JPC activated with OB-medium or OB/BMP-2 (Fig. 5b, c). Beside the greatly stronger JPC proliferation after induction of osteogenesis and the multilayered cell growth, a specific nodule formation was observed in 3D-constructs differentiated with OB-medium and with OB/BMP-2. Element analysis using EDX spectrometry clarified the chemical nature of these particles. Some analyzed particles showed calcium and phosphorus as considerable fraction (Fig. 5d, upper panel). However, much more analyzed particles were mainly composed of calcium (Fig. 5d, lower panel).

3.5 Analysis of gene expression of JPC-seeded OPLA scaffolds after induction of osteogenesis

O_2-measurements of JPC-seeded 3D-constructs showed the highest proliferation after day 12 of in vitro culturing. Therefore, we chose this time point for gene expression analysis of JPC-seeded OPLA scaffolds (Table 1, $n = 3$).

JPC treated with OB-medium and OB/BMP-2 showed strongly induced transcription levels (4 to 20-fold) of alkaline phosphatase compared with standard medium. However, activation with BMP-2 did not lead to a further activation of AP.

In contrast to AP, gene expression levels of Runx-2 seemed to be further activated through BMP-2. Whereas OB-treated JPC showed a 1.6 to 3.7-fold induction in comparison to untreated cells, differentiating JPC additionally stimulated with BMP-2 showed 2.3 to 6.3-fold higher transcription levels of Runx-2. Likewise, osterix

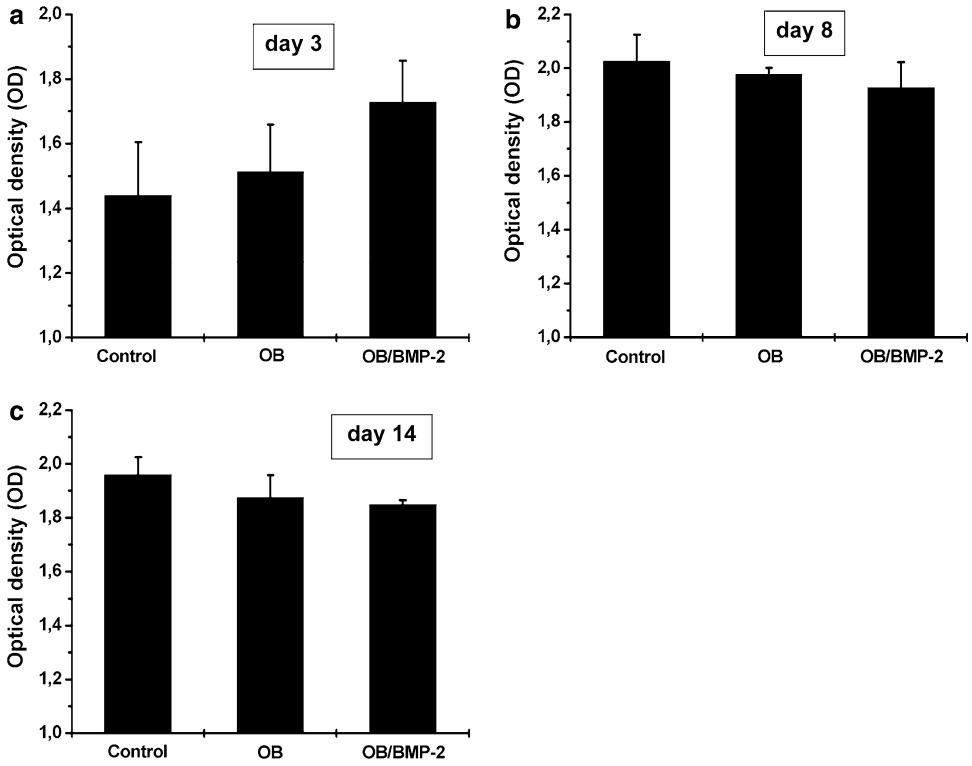

Fig. 4 JPC proliferation rates within OPLA scaffolds ($n = 3$). JPC were seeded into OPLA scaffolds and JPC osteogenesis was started by addition of OB-medium and OB/BMP-2 respectively. Metabolic activity was measured after day 3 (**a**), day 8 (**b**) and day 14 (**c**) of in vitro 3D-culturing by a colorimetric assay. Optical densities (OD) are denoted in the Y-axis

gene expression (Osx) seemed to be also BMP-2 susceptible. JPC treated with OB-medium showed only a weak induction of Osx mRNA copy numbers. In contrast, in OB/BMP-2 stimulated cells an activation of up to 32-fold of this gene was detected, however in general, osterix expression levels remained very low.

Analysis of insulin-like growth factor-1α (IGF-1α) expression revealed a repression of this gene (data not shown), whereas a strong induction of IGF-2 transcript levels was observed during JPC osteogenesis. In OB-treated cells we found a 4.3 to 23-fold higher mRNA copy number and a 6 to 34-fold induction of IGF-2 in OB/BMP-2 activated JPC in comparison to untreated JPC. Osteocalcin and osteopontin gene expression analysis showed no significant difference in comparison to control JPC (data not shown).

3.6 Detection of alkaline phosphatase within JPC-seeded OPLA scaffolds

Addition of the substrate naphthol AS-MX phosphate and fast violet B salt to the JPC-seeded OPLA-scaffolds revealed strong differences between OPLA scaffolds cultured in standard medium, OB-medium or OB/BMP-2 (Fig. 6, $n = 3$). While OPLA-scaffolds containing untreated JPC in standard medium remained nearly unstained, 3D-constructs containing differentiating JPC in OB-medium and OB/BMP-2 showed a strong positive reaction (reddish dye). Semiquantitative staining revealed no differences between OB-medium and OB/BMP-2 corresponding to gene expression data.

4 Discussion

In the present study, we examined 3D OPLA scaffolds for their growth and osteoinductive potential for human jaw periosteal cells (JPC). Between commercially available collagen (Coll), open-cell polylactic acid (OPLA) and calcium phosphate (CaP) 3D-scaffolds, OPLA seemed to be the most beneficial for human JPC growth at all analyzed time points.

Analysis of proliferation rates by classical determination of cell numbers lacks on a sufficient yield of detachable cells from the scaffolds. Therefore, we used two approaches to measure proliferation rates within the scaffolds. JPC proliferation tests within the three different scaffolds (Coll, OPLA and CaP, Fig. 1) reflect the real proliferation rates due to the same metabolic activity of the cells—they were all treated with standard medium. Analysis of proliferation during the osteogenesis process resulted in weak differences between the untreated and both differentiated groups. In contrast to our proliferation test, scanning electron micrographs clearly showed a denser and multilayered colonization of OPLA scaffolds after initiation of

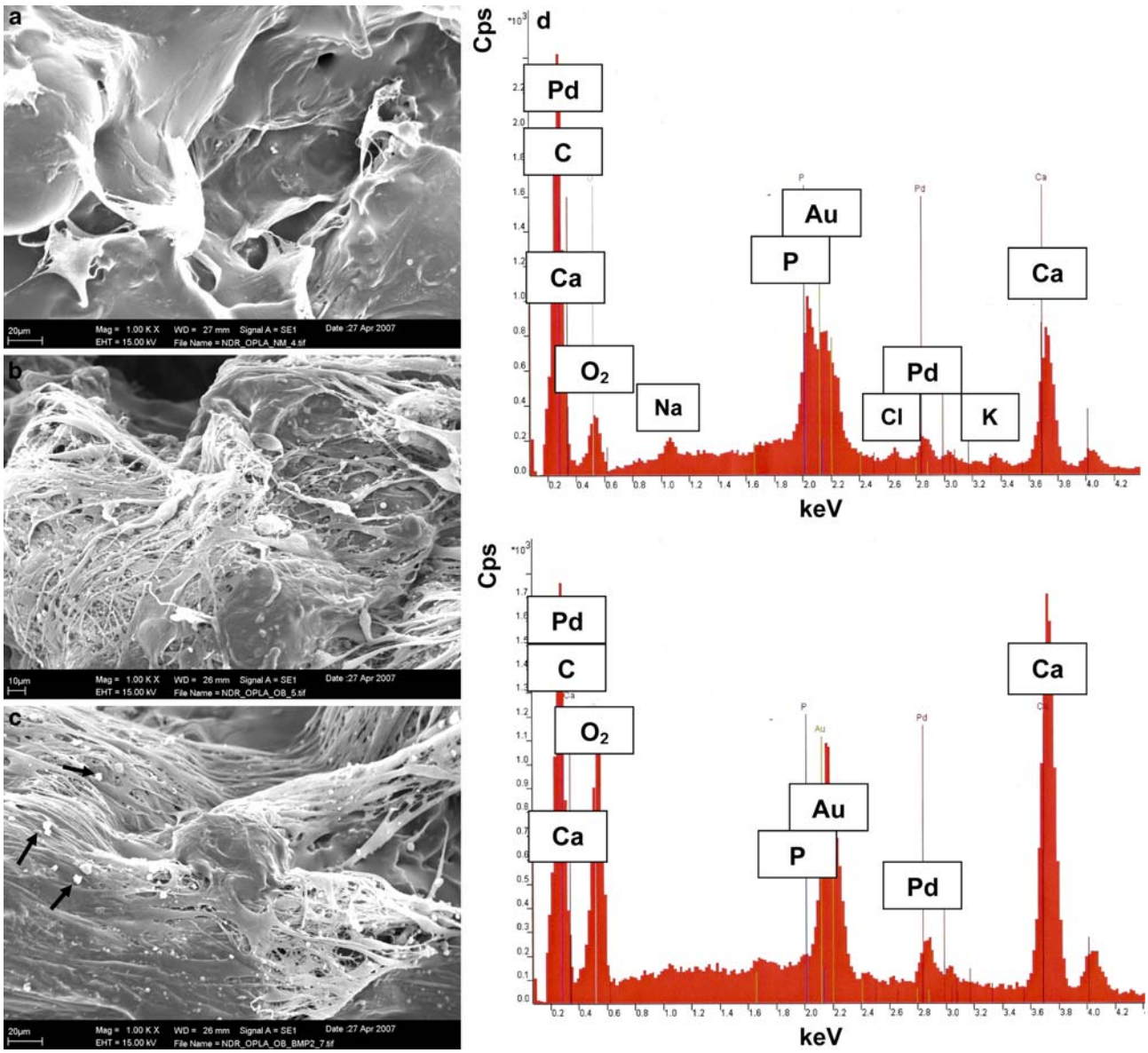

Fig. 5 Scanning electron micrographs (SEMs) of untreated and differentiating JPC seeded within OPLA scaffolds. Untreated JPC showed a weak colonization on the surface of OPLA scaffolds (**a**) in comparison to JPC treated with OB-medium or with OB/BMP-2 (**b**, **c**). SEMs are illustrated in a 1000-fold magnification. Furthermore, JPC seeded within OPLA scaffolds revealed a specific nodule formation (**c**, black arrows) under differentiating conditions after 13–14 days of in vitro culturing (**b**, **c**). Representative element analysis of formed particles by EDX spectrometry is illustrated in (**d**) (Au and Pd peaks are caused by sputter coating of samples). X-axis denotes kiloelectron volt (keV) and y-axis denotes counts per second (cps)

osteogenesis (Fig. 5a–c). This suggests that our proliferation test measures the metabolic activity, but is not able to detect the real proliferation rates of differentiating JPC. During osteogenesis JPC were strongly proliferated whereas metabolic activity was downregulated as indicated by the test.

Furthermore, using a new approach, we were able to continually measure oxygen concentrations within each well containing cell-seeded 3D-scaffolds during 15 days of in vitro culturing. We found the highest oxygen consumption between 12–14 days of in vitro culturing. After this time point, oxygen concentrations increased again, suggesting that JPC probably undergo apoptosis. These results indicate that the in vitro culturing time within the 3D-constructs should not exceed 12–14 days, but rather fall below this time limit. Oxygen measurements were determined within 24-well plates in a relatively high volume of culture medium. Therefore, the limitation of this test is that alterations in oxygen concentrations could be obliterated.

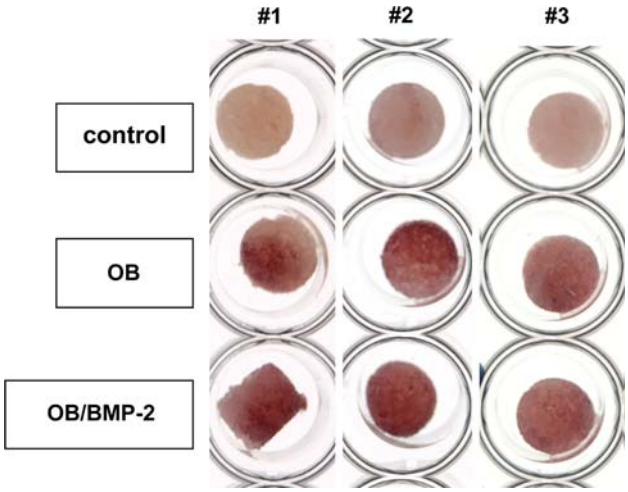

Fig. 6 Detection of AP within OPLA scaffolds after 13–14 days of in vitro culturing ($n = 3$). JPC were seeded within OPLA scaffolds. After 13–14 days of in vitro culturing, untreated (control) and differentiating JPC (OB-medium and OB/BMP-2) were stained with the naphthol-phosphate substrate for detection of AP activity. Scaffolds containing untreated JPC remained unstained whereas constructs containing differentiating JPC exhibited a reddish dye

We chose the time of highest proliferation (day 12) for gene expression analysis to examine whether the osteogenesis process was already initiated. Due to low proliferation rates and insufficient RNA yield within collagen and CaP scaffolds, we could only analyze gene expression of differentiating JPC seeded on OPLA scaffolds. The reason for the weak proliferation of JPC seeding within collagen and CaP scaffolds in our experiments is not clear, despite of their known suitability for osteoblasts. A possible explanation for this effect could be due to different composition of the used collagen scaffolds (mixture of type I and III collagen), which is probably less suitable for JPC or differences during manufacturing of the used CaP scaffolds.

While RNA isolation from cell-seeded 3D-constructs remained tricky so far, we established a new approach for quick and efficient disruption of 3D-constructs using the MagNa Lyser instrument. Using this method, cells growing within the scaffolds are not enzymatically manipulated for a long time, but gene expression levels reflect the instantaneous situation. Induction of osteogenesis-relevant genes was detected by quantitative real-time PCR, indicating that this time point may be sufficient for the in vitro initiation of osteogenesis. The transcription factor osterix is critical for both skeletogenesis and osteoblast differentiation [17–19]. It regulates transcription down-stream of Runx-2/Cbfa1 during skeletal development [19]. Insulin-like growth factor was already described as regulator of the anabolic activity of parathyroid hormone on mouse bone [20] as well as inducer of osteoprogenitor cell proliferation [21].

BMP-2 is known to stimulate and to shorten the time course of osteogenesis of periosteum-derived cells [22]. Our PCR data support the hypothesis, that BMP-2 intensifies the osteogenic differentiation process of periosteal cells by further enhancement of the analyzed genes in comparison to differentiating JPC cultured in the absence of the recombinant protein. Additionally, we demonstrated by EDX spectrometry that differentiating JPC within OPLA scaffolds are able to build Ca precipitates even though only a small part of them in the form of CaP. This may be due to incomplete JPC differentiation after day 13–14 of 3D-culturing. In the 2D-culture system, cells need 20–21 days to completely mineralize.

Choose of the suitable stem cell type remains a further challenge for bone regeneration research. The comparison of the chondrogenic potential of mesenchymal stem cells isolated from periosteum, bone marrow or fat of adult rats lead to the conclusion that periosteum- and bone marrow derived cells seem to be superior to cells isolated from fat with respect to forming cartilaginous tissue [23]. On the other site the comparison of the osteogenic capacity of human JPC and mesenchymal stem cells from bone marrow (BMMSC) indicate that BMMSC are superior to JPC concerning this [24]. Recently published, Agata et al. found that pre-treatment of periosteal cells with basic fibroblast growth factor (b-FGF) made them more sensitive to BMP-2 and more osteogenic [25]. Transplants of periosteal cells treated with BMP-2 after pre-stimulation with b-FGF formed more new bone than marrow stromal cells did [26]. Periosteal cells are of interest for tissue engineering applications because of their advantages compared to BMMSC. The potential for sufficient proliferation of periosteal cells has been demonstrated in elderly individuals and may persist throughout life. It has been concluded that the mineralization potential of periosteal cells is not age dependent [26, 27]. In contrast, the number of progenitors in bone marrow is thought to decline with age [28–30]. Furthermore the harvest of JPC is simple and causes minimal morbidity. Schmelzeisen et al. published in a preliminary report a successful bone augmentation of the posterior maxilla using polymer fleeces and pre-differentiated periosteal cells [31].

It remains difficult to meet all demands of bone regeneration. The high degree of variability in form and function of bone suggests that not only one solution will be optimal for different clinical applications and defect sites. The porosity of bone varies from approximately 5% in cortical bone to over 90% in trabecular bone regions. The forces applied to bone are partially negligible in calvarial and midfacial bones. In contrast, the mandible, long bones in the lower limb and articular joints have to withstand higher forces.

The establishment of procedures for the isolation, phenotypic and functional characterization of used stem cells and suitable scaffolds are paramount for the subsequent application for cell transplantation.

5 Conclusion

In our study, JPC growing within open-cell polylactic acid scaffolds showed the highest proliferation rates among the analyzed scaffold types. Scanning electron micrographs illustrated the denser colonization of JPC-seeded OPLA scaffolds and formation of nodules after initiation of osteogenesis. EDX spectrometry demonstrated that JPC growing within OPLA scaffolds are able to form CaP particles.

To our knowledge, the analyzed open-cell polylactic acid scaffolds provide a promising environment for bone substitutes using human JPC. Further studies remain to elucidate the osteoconductivity of this scaffold type in vivo.

Acknowledgements The authors acknowledge the excellent technical assistance of Günter Wedenig.

References

1. C. DE BARI, F. DELL'ACCIO and F. P. LUYTEN, *Arthritis Rheum.* **44** (2001) 85
2. C. DE BARI, F. DELL'ACCIO, J. VANLAUWE, J. EYCKMANS, I. M. KHAN, C. W. ARCHER, E. A. JONES, D. MCGONAGLE, T. A. MITSIADIS, C. PITZALIS and F. P. LUYTEN, *Arthritis Rheum.* **54** (2006) 1209
3. H. NAKAHARA, S. P. BRUDER, S. E. HAYNESWORTH, J. J. HOLECEK, M. A. BABER, V. M. GOLDBERG and A. I. CAPLAN, *Bone* **11** (1990) 181
4. H. NAKAHARA, V. M. GOLDBERG and A. I. CAPLAN, *J. Orthop. Res.* **9** (1991) 465
5. K. MURAMATSU and A. T. BISHOP, *J. Orthop. Res.* **20** (2002) 772
6. C. N. CORNELL, *Orthop. Clin. North Am.* **30** (1999) 591
7. P. DUCHEYNE, A. EL-GHANNAM and I. SHAPIRO, *J. Cell. Biochem.* **56** (1994) 162
8. H. M. ELGENDY, M. E. NORMAN, A. R. KEATON and C. T. LAURENCIN, *Biomaterials* **14** (1993) 263
9. D.W. HUTMACHER, *Biomaterials* **21** (2000) 2529
10. C. T. LAURENCIN, M. A. ATTAWIA, H. E. ELGENDY, K. M. HERBERT, Bone **19** (1996) 93S
11. J. F. MANO, G. A. SILVA, H. S. AZEVEDO, P. B. MALAFAYA, R. A. SOUSA, S. S. SILVA, L. F. BOESEL, J. M. OLIVEIRA, T. C. SANTOS, A. P. MARQUES, N. M. NEVES and R. L. REIS. *Soc. Interface* **4**(17) (2007) 999
12. A. G. MIKOS, G. SARAKINOS, S. M. LEITE, J. P. VACANTI and R. LANGER, *Biomaterials* **14** (1993) 323
13. Y. MOHAMMADI, M. SOLEIMANI, M. FALLAHI-SICHANI, A. GAZME, V. HADDADI-ASL, E. AREFIAN, J. KIANI, R. MORADI, A. ATASHI and N. AHMADBEIGI, *Int. J. Artif. Organs* **30** (2007) 204
14. L.A. SOLCHAGA, J. E. DENNIS, V. M. GOLDBERG and A. I. CAPLAN, *J. Orthop. Res.* **17** (1999) 205
15. L.G. GRIFFITH, *Ann. NY Acad. Sci.* **961** (2002) 83
16. V. KARAGEORGIOU and D. KAPLAN, *Biomaterials* **26** (2005) 5474
17. G. LEVI, V. GEOFFROY, G. PALMISANO, M. C. DE VERNEJOUL, EMBO Rep. **3** (2002) 22
18. N. HOLLEVILLE, A. QUILHAC, M. BONTOUX and A. H. MONSORO-BURQ, *Dev. Biol.* **257** (2003) 177
19. M. H. LEE, T. G. KWON, H. S. PARK, J. M. WOZNEY and H. M. RYOO, *Biochem. Biophys. Res. Commun.* **309** (2003) 689
20. D. D. BIKLE, T. SAKATA, C. LEARY, H. ELALIEH, D. GINZINGER, C. J. ROSEN, W. BEAMER, S. MAJUMDAR and B. P. HALLORAN, *J. Bone Miner. Res.* **17** (2002) 1570
21. Y. KASUKAWA, L. STABNOV, N. MIYAKOSHI, D. J. BAYLINK, and S. MOHAN, *J. Bone Miner. Res.* **17** (2002) 1579
22. M. IWASAKI, H. NAKAHARA, T. NAKASE, T. KIMURA, K. TAKAOKA, A. I. CAPLAN and K. ONO, *J. Bone Miner. Res.* **9** (1994) 1195
23. J. PARK, K. GELSE, S. FRANK, K. VON DER MARK, T. AIGNER and H. SCHNEIDER, *J. Gene. Med.* **8** (2006) 112
24. C. J. AQUIERY, S. SCHAEREN, J. F. ARHADI, P. MAINIL-VARLET, C. KUNZ, H. F. ZEILHOFER, M. HEBERER and I. MARTIN, *Ann. Surg.* **242** (2005) 859, discussion
25. H. AGATA, I. ASAHINA, Y. YAMAZAKI, M. UCHIDA, Y. SHINOHARA, M. J. HONDA, H. KAGAMI and M. UEDA, *J. Dent. Res.* **86** (2007) 79
26. H. AGATA, I. ASAHINA, Y. YAMAZAKI, M. UCHIDA, Y. SHINOHARA, M. J. HONDA, H. KAGAMI and M. UEDA, *J. Dent. Res.* **86** (2007) 79
27. Y. KOSHIHARA, M. KAWAMURA, S. ENDO, C. TSUTSUMI, H. KODAMA, H. ODA and S. HIGAKI, *In Vitro Cell Dev. Biol.* **25** (1989) 37
28. G. F. MUSCHLER and R. J.MIDURA, *Clin. Orthop. Relat Res.* (395) (2002) 66
29. G. D'IPPOLITO, P. C. SCHILLER, C. RICORDI, B. A. ROOS and G. A. HOWARD, *J.Bone Miner.Res.* **14** (1999) 1115
30. B. A. HUIBREGTSE, B. JOHNSTONE, V. M. GOLDBERG and A. I. CAPLAN, *J. Orthop. Res.* **18** (2000) 18
31. R. SCHMELZEISEN, R. SCHIMMING and M. SITTINGER, *J. Craniomaxillofac. Surg.* **31** (2003) 34